Supporting Material for

Multiplane Quantitative Phase Imaging Using a Wavelength-Multiplexed Diffractive Optical Processor

Che-Yung Shen[1,2,3], Jingxi Li[1,2,3], Yuhang Li[1,2,3], Tianyi Gan[1,3], Langxing Bai [4], Mona Jarrahi[1,3] and Aydogan Ozcan[1,2,3*]

[1]Electrical and Computer Engineering Department, University of California, Los Angeles, CA, 90095, USA

[2]Bioengineering Department, University of California, Los Angeles, CA, 90095, USA

[3]California NanoSystems Institute (CNSI), University of California, Los Angeles, CA, 90095, USA

[4]Department of Computer Science, University of California, Los Angeles, CA, 90095, USA

[*]Correspondence to: ozcan@ucla.edu

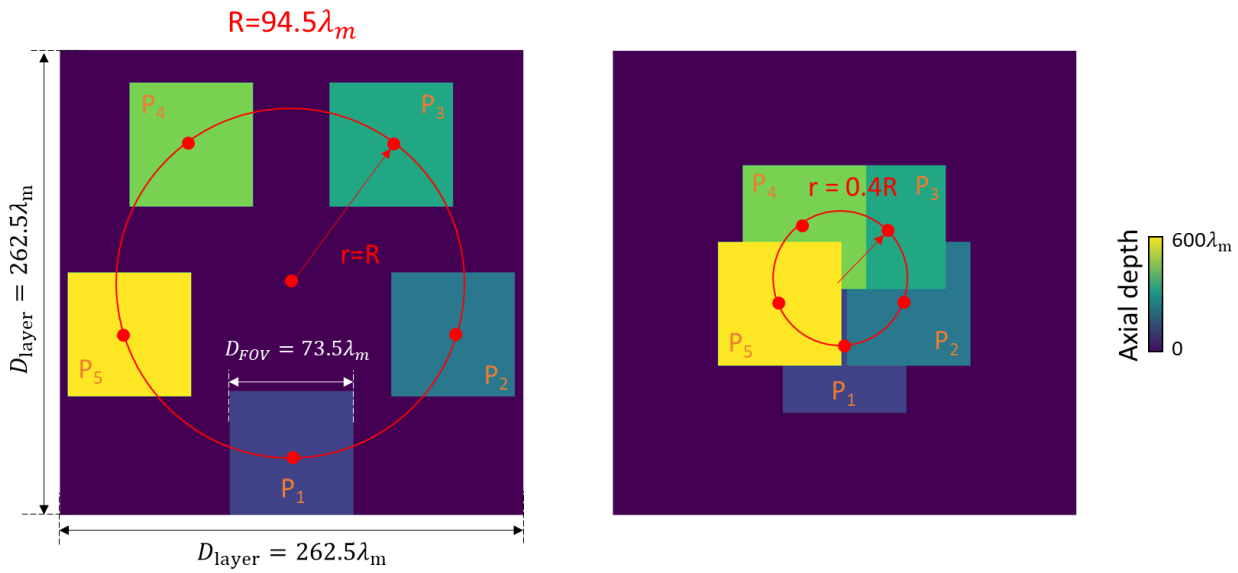

Figure S1. Visualization of the distribution of the separated input objects (located at different axial planes) for the diffractive multiplane QPI processor. Each input object is spatially separated with the input lateral separation distance r from the center of the optical axis to the center of each input object.

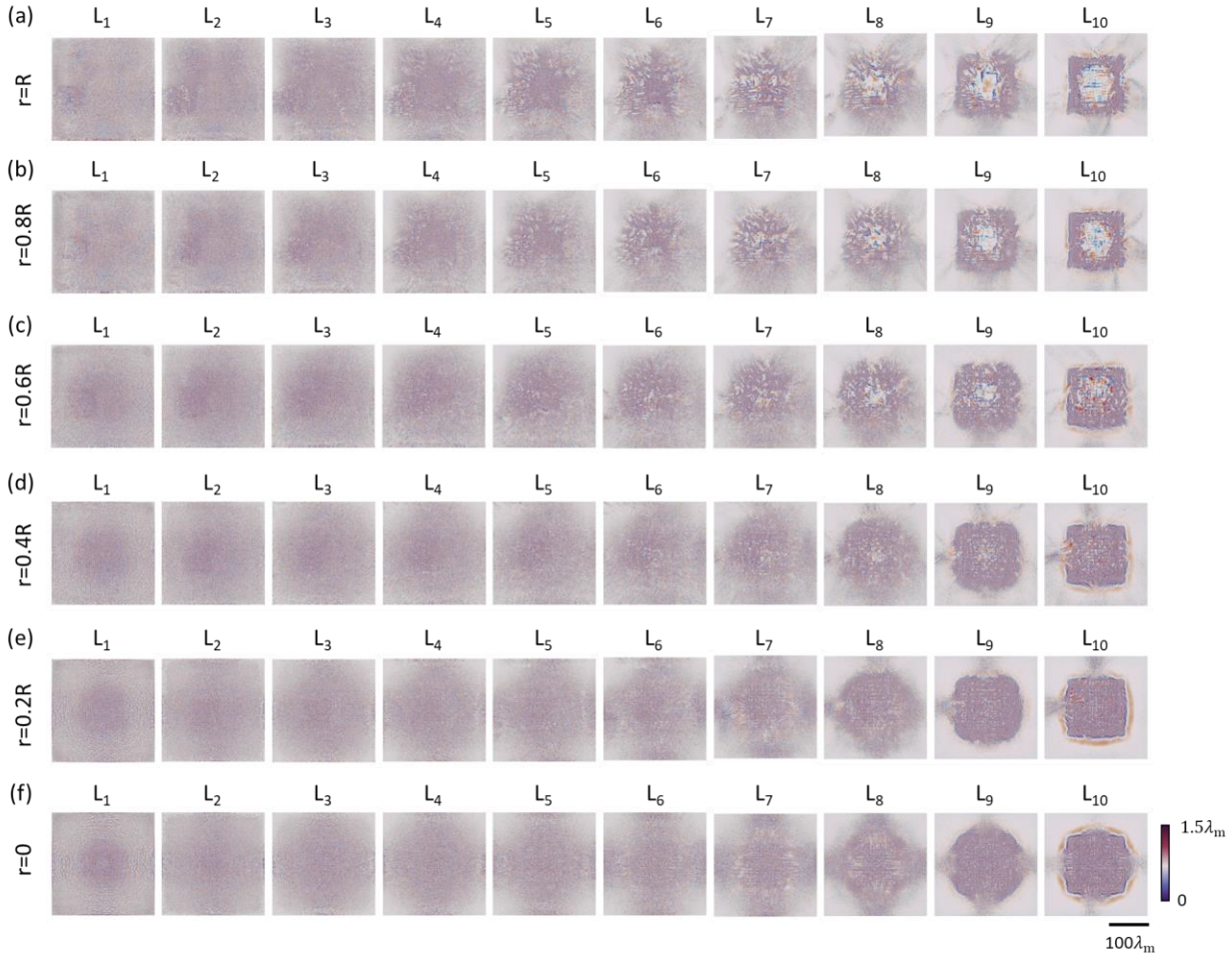

Figure S2. Diffractive multiplane QPI designs with different input lateral separation distances (r). Here, the six diffractive designs were trained under the same configurations, except for using different input lateral separation distances (r) covering {0, 0.2R, 0.4R, 0.6R, 0.8R, R}.

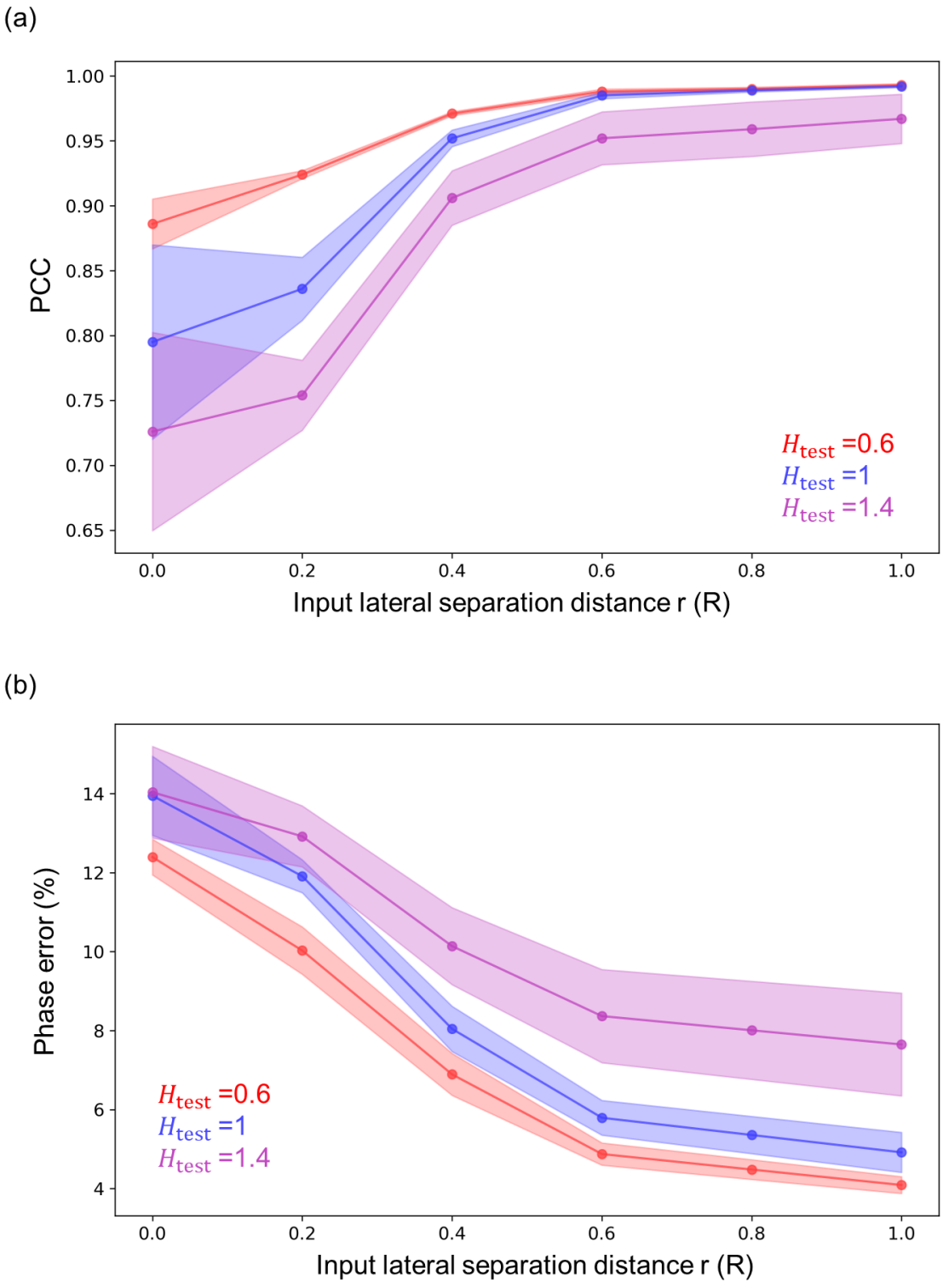

Figure S3. Impact of the input lateral separation on the multiplane QPI performance. a, Average PCC values as a function of the input lateral separation distance. **b,** Average phase MAE as a function of the input lateral separation distance. These curves refer to the blind testing performance under different testing thickness range parameters (H_{test}).

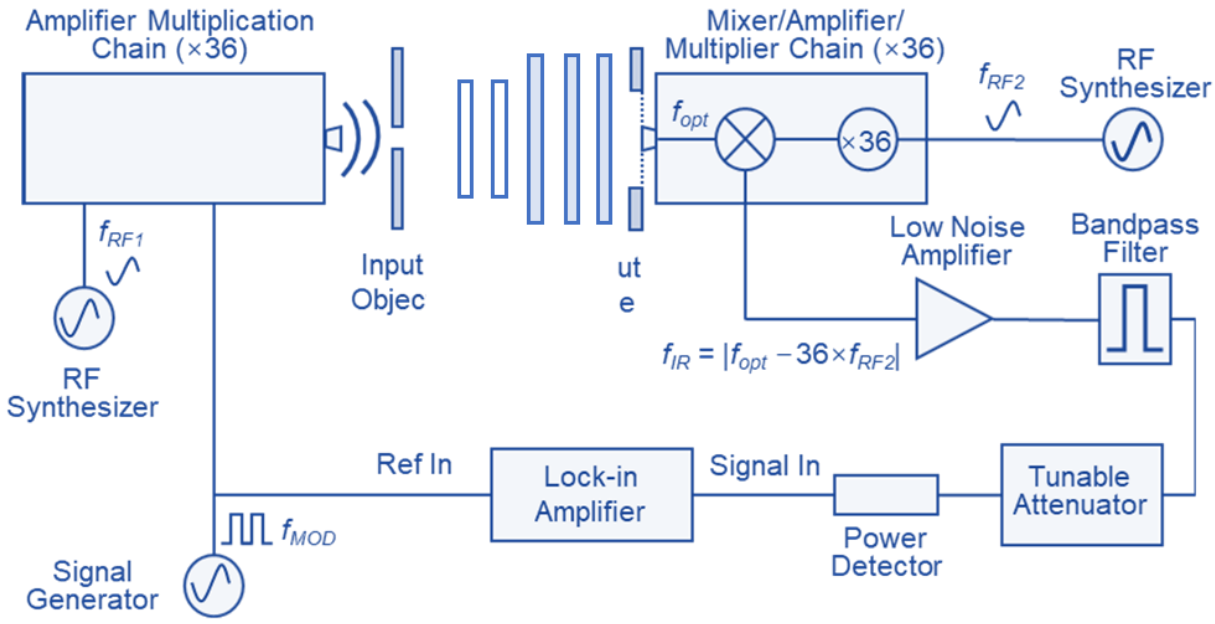

Figure S4. Schematics of the experimentally used terahertz imaging set-up.

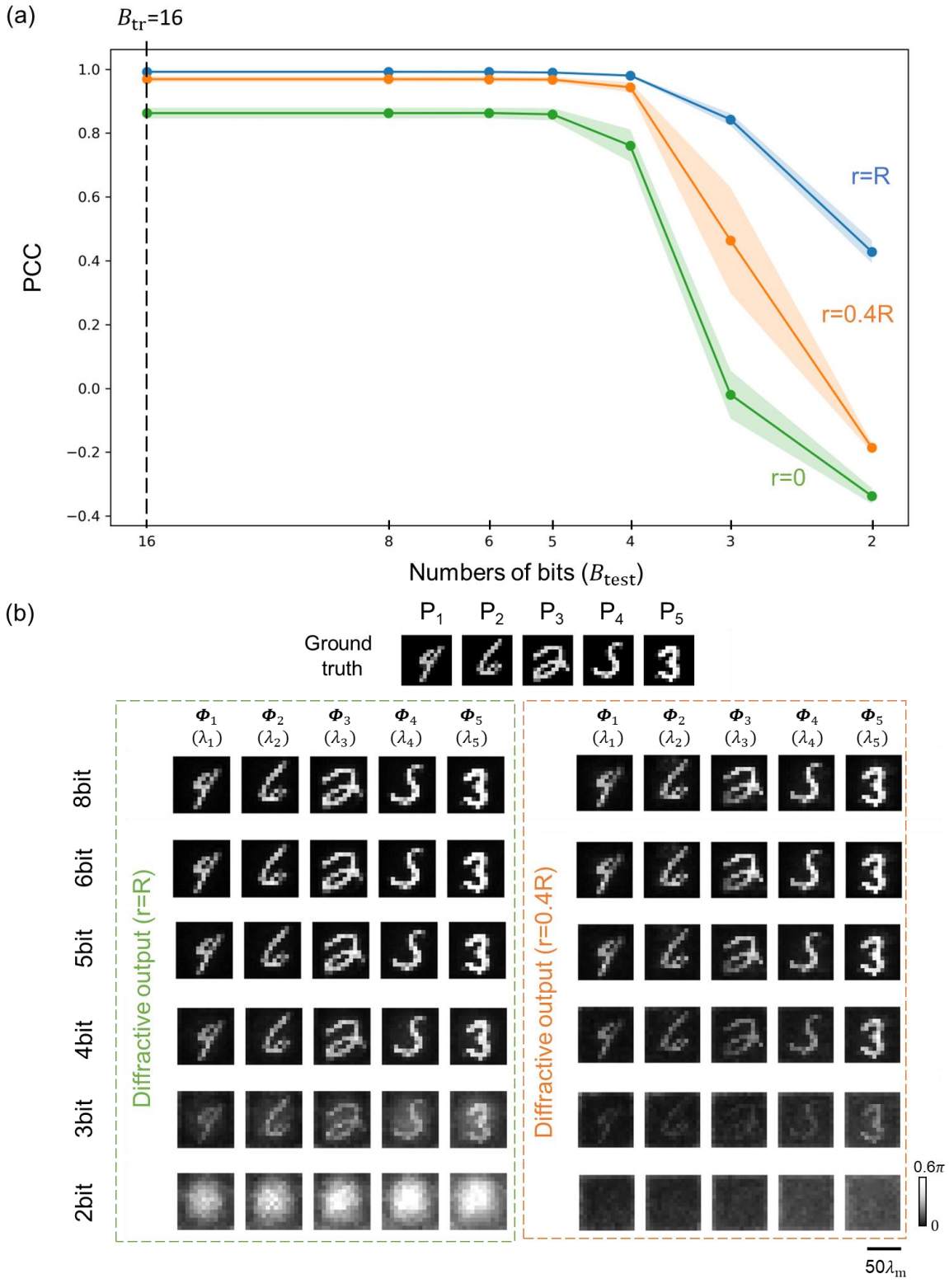

Figure S5. Impact of the phase quantization level of the diffractive layers on the multiplane QPI performance. a, PCC values as a function of different phase quantization levels in a range

of {16, 8, 6, 5, 4, 3, 2} bits. **b,** Examples of the diffractive multiplane QPI output images demonstrated for different phase quantization levels.

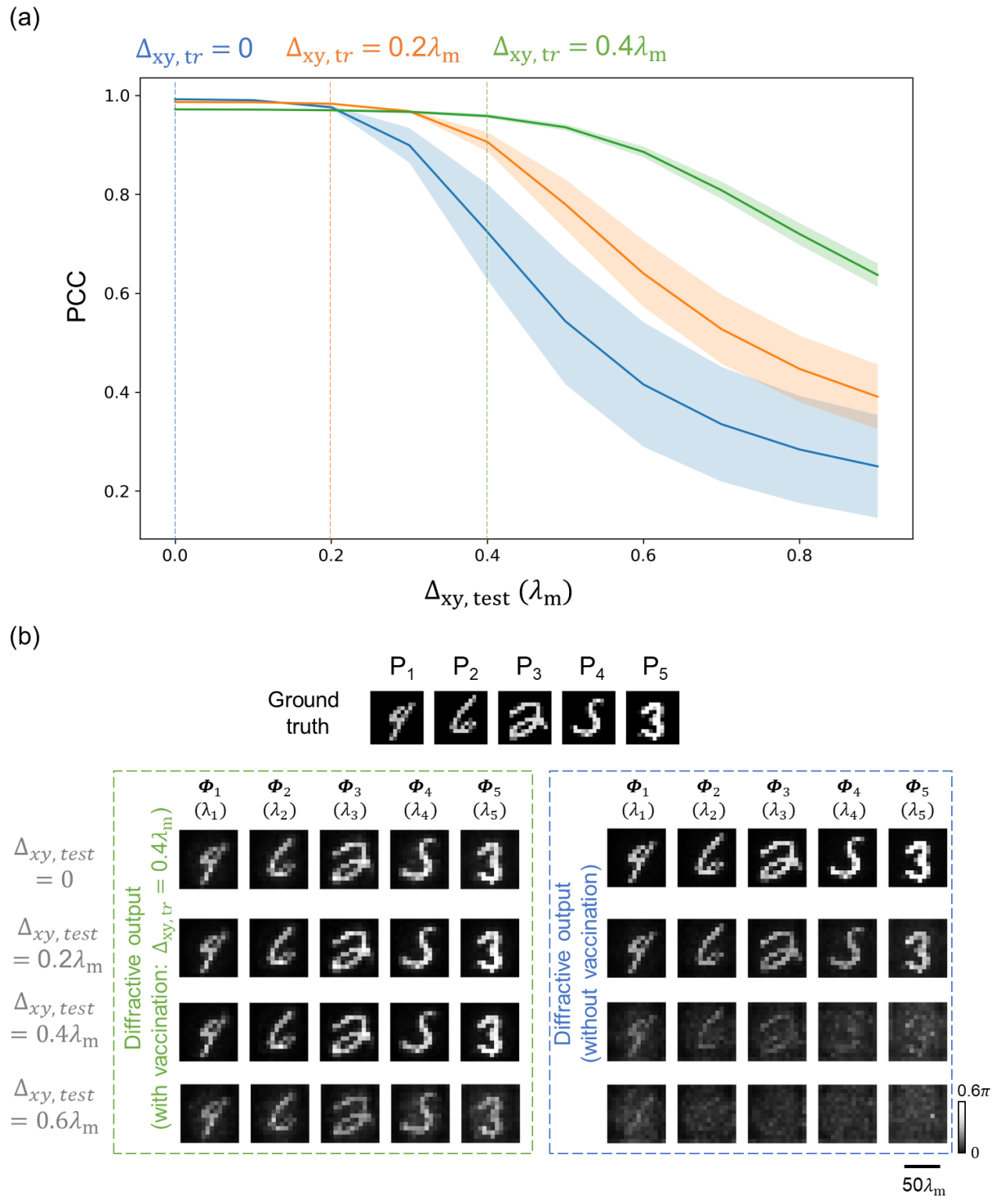

Figure S6. Impact of lateral misalignments on the QPI performance of the vaccinated r=R diffractive multiplane QPI processors. a, PCC values of the diffractive QPI processor outputs as a function of random lateral shifts. The blue curves represent the performance of the diffractive QPI processor previously shown in **Fig. S2a** in the **Supplementary Material**; the other curves (green and orange) represent the vaccinated diffractive QPI processor designs. **b,** Examples of the

diffractive QPI output images demonstrated with or without vaccination under different levels of testing lateral misalignments.

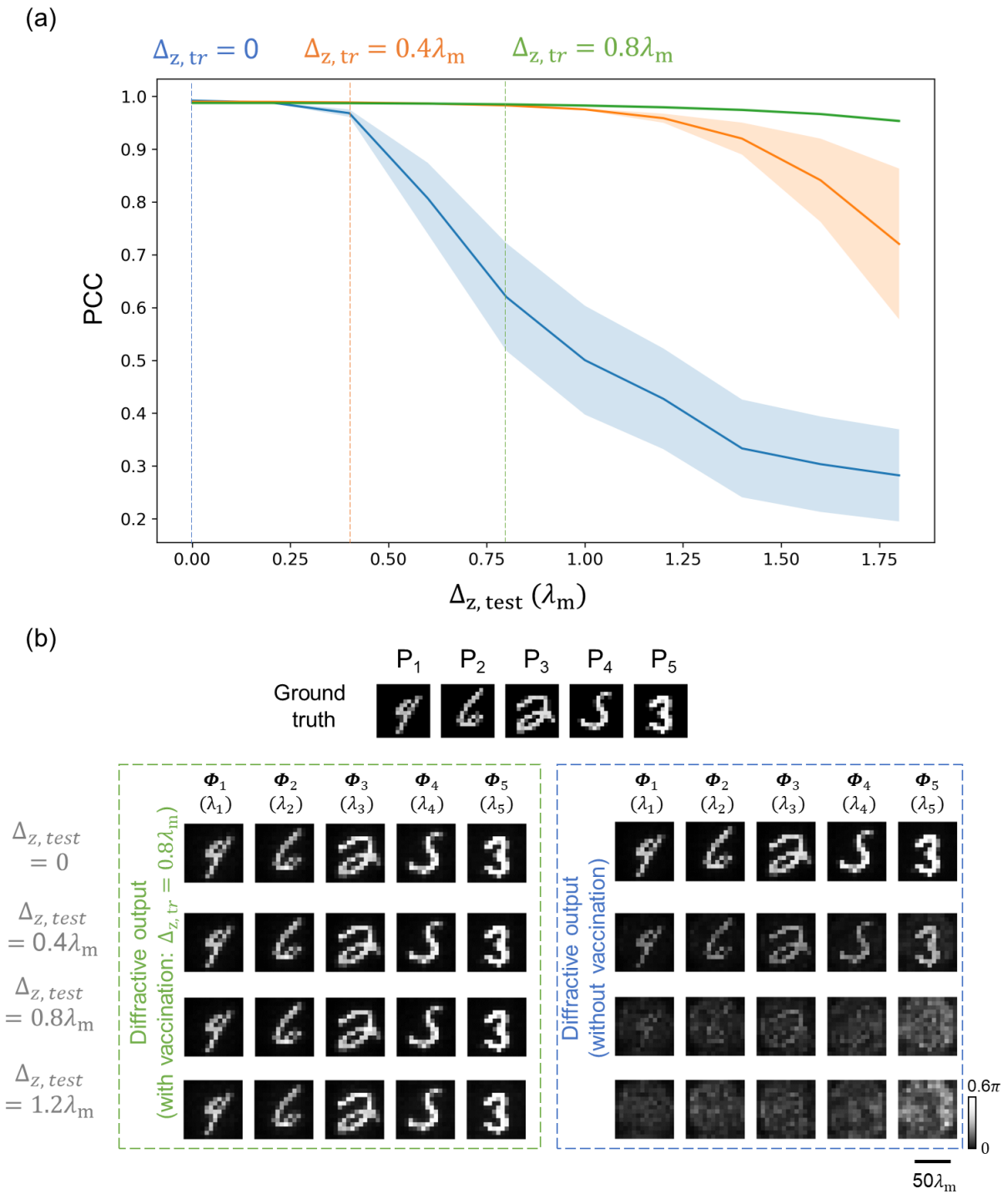

Figure S7. Impact of axial misalignments on the QPI performance of the vaccinated r=R diffractive multiplane QPI processors. a, PCC values of the diffractive QPI processor outputs as a function of random axial shifts. **b,** Examples of the diffractive QPI output images demonstrated with or without vaccination under different levels of testing axial misalignments.

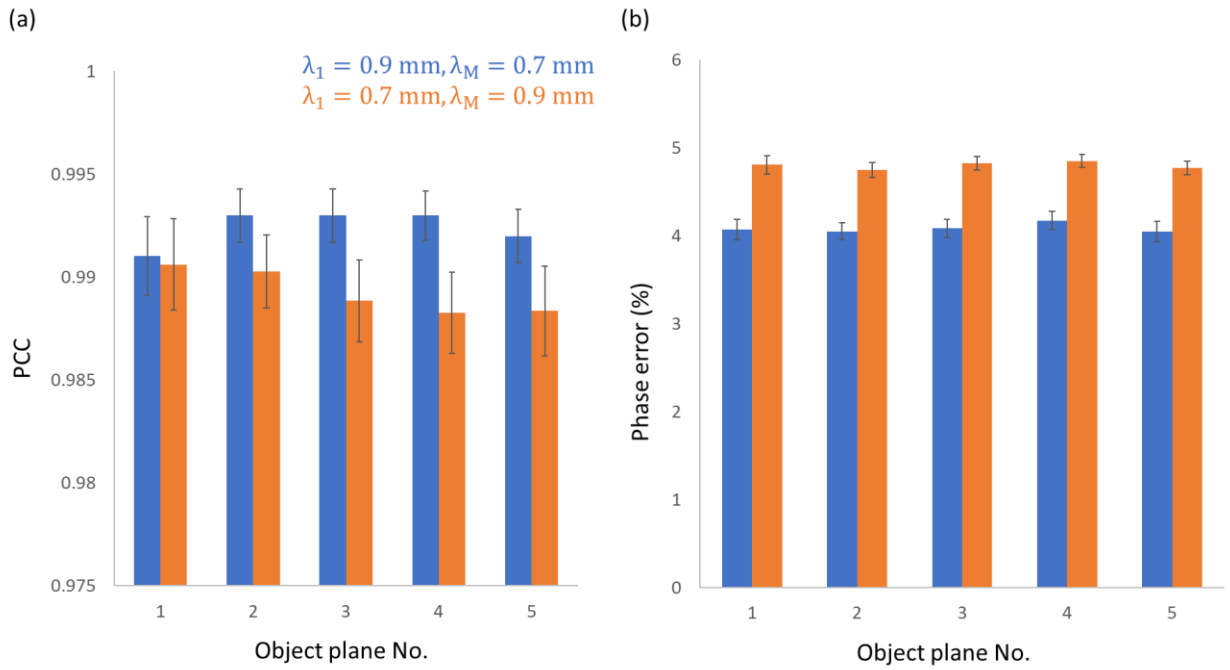

Figure S8. Impact of different channel assignment strategies on multiplane QPI performance of the r = R diffractive multiplane QPI processor design. The blue bars illustrate the multiplane QPI performance using our wavelength assignment strategy, which assigns shorter wavelengths to the later/deeper input planes, and the orange bars show the multiplane QPI performance with the reversed wavelength assignment, i.e., longer wavelengths are assigned to the later/deeper input planes. **a,** PCC values of the resulting multiplane QPI performance with $H_{\text{test}} = 0.6$ under different wavelength assignments. **b,** Phase MAE values of the resulting multiplane QPI measurements with $H_{\text{test}} = 0.6$ under different wavelength assignments.

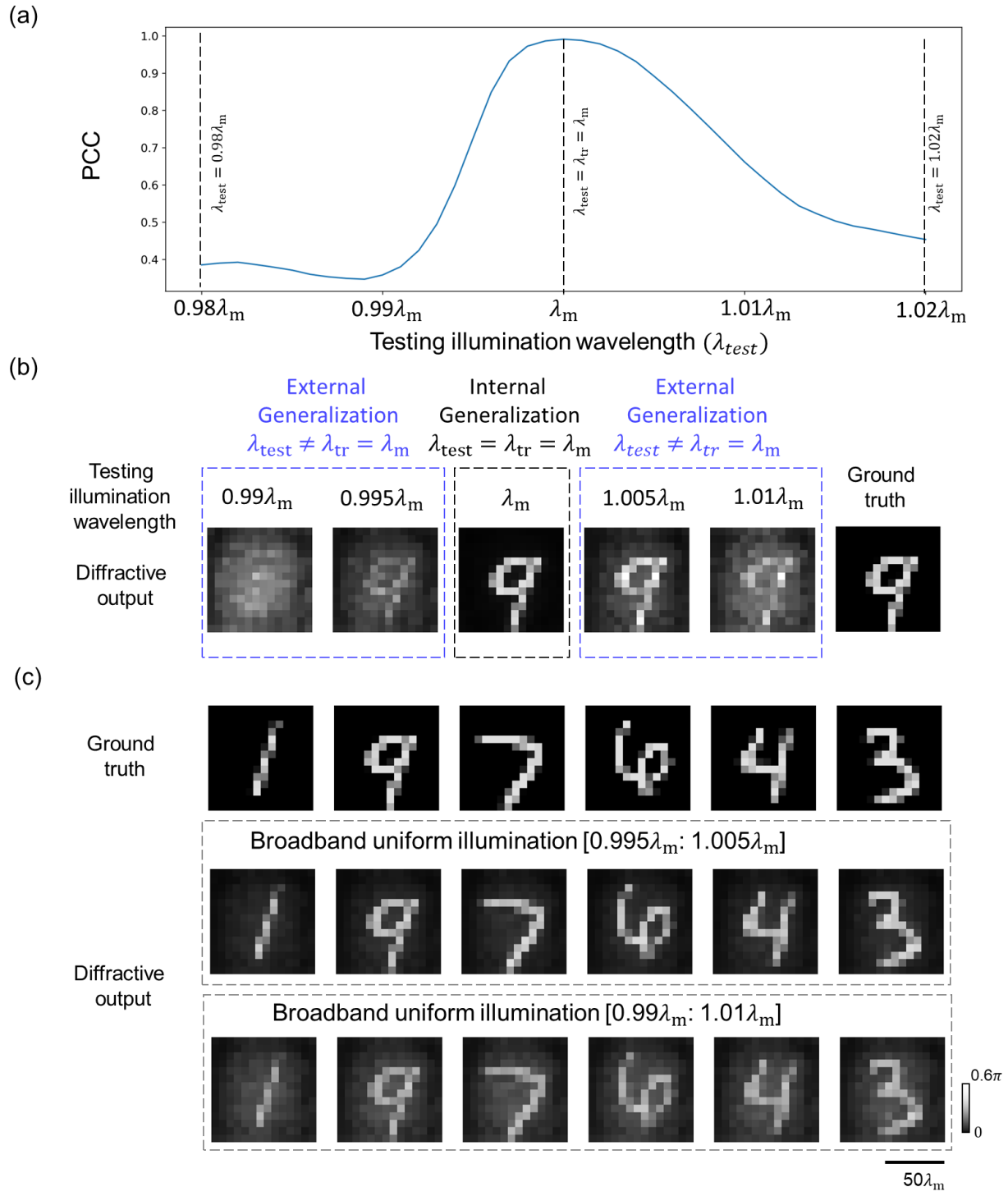

Figure S9. Spectral response of the r=R diffractive multiplane QPI processor. a, PCC values as a function of the testing illumination wavelength. **b,** Examples of the diffractive QPI output images when using different testing illumination wavelengths. **c,** Examples of the diffractive QPI output images under two different broadband illumination cases, uniformly covering [$0.995\lambda_m$: $1.005\lambda_m$] and [$0.99\lambda_m$: $1.01\lambda_m$].